JOURNAL OF GUIDANCE, CONTROL, AND DYNAMICS
Vol. 17, No. 4, July–August 1994

Comparison of Low-Earth-Orbit Satellite Attitude Controllers Submitted to Controllability Constraints

Willem H. Steyn*
University of Stellenbosch, Stellenbosch 7600, South Africa

A rule-based fuzzy controller is presented and compared with an adaptive MIMO LQR controller in a low-Earth-orbit small satellite attitude control system. The attitude is passively gravity gradient stabilized and actively three-axis magnetorquer controlled. This method insures an Earth-pointing satellite making use of a nondepletable and nonmechanical means of control. A realistic simulation environment, using a nonlinear satellite dynamic model with linear attitude estimators plus sensor measurement noise and external disturbance torques, was used to evaluate the different control techniques.

I. Introduction

SMALL low-cost satellites are becoming more important in the last few years when the possibility of piggyback launch opportunities, e.g., the Ariane Structure for Auxiliary Payloads (ASAP), and smaller commercial launchers like Pegasus became available. The aim of this control system is to achieve a stable Earth-pointing attitude, maximizing the pointing accuracy and minimizing the control energy, within the limitation of the existing low-cost technology. A possible resource to be explored for improved performance of future low-cost satellites is the processing capability of onboard microprocessors. Innovative attitude control theory, more explicitly discrete time estimators, and control laws can be used to obtain this goal.

As an example, a small satellite controller, making use of a gravity gradient boom (Fig. 1) and magnetic coils (magnetorquers) to maintain an Earth-pointing attitude, while either slowly spinning around its nadir axis or maintaining a reference yaw angle, will be designed. The orbit will be near circular and polar (sun synchronous) at an approximately 800-km altitude. The only sensor mandatory for magnetorquing is a magnetometer; the other attitude sensors can be of any low-cost type, e.g., Earth horizon and sun sensors. The remainder of the introduction will give a quick overview of the relevant material needed before the proposed controllers can be presented.

Magnetorquing

Magnetic coils around the spacecraft's *XYZ* axes (Fig. 1) can be fed with a constant current—switched in two directions—to generate a magnetic dipole moment $\boldsymbol{M}$. This will interact with the geomagnetic field vector $\boldsymbol{B}$ to generate a torque $\boldsymbol{N}$ by taking the cross product:

$$\boldsymbol{N} = \boldsymbol{M} \times \boldsymbol{B} \tag{1}$$

Although the direction and magnitude of $\boldsymbol{M}$ can be controlled on average by the correct interleaving of the three magnetic coils, the $\boldsymbol{B}$ vector is totally dependent on the orbital location. As a result, the torque $\boldsymbol{N}$ will always be orthogonal to $\boldsymbol{B}$ (and $\boldsymbol{M}$) and not favorable in certain regions of the orbit to control the attitude of a specific spacecraft axis. It is also possible that a desirable control torque around an attitude axis (pitch, roll, or yaw), when a specific coil or a combination of magnetic coils is switched, will generate undesired disturbance torques on the other axes. The main objective of the control algorithm will therefore be to optimize the control effort: maximize the desired influence and minimize the undesired disturbances.

Geomagnetic Field Vector

This vector can be modeled in orbital plane components B_{X0}, B_{Y0}, and B_{Z0} where the X_0 axis is along the velocity vector, the Y_0 axis is normal to the orbit plane, and the Z_0 axis is toward the Earth's center (nadir direction). The vector components can be obtained from an International Geomagnetic Reference Field (IGRF) model[1] or a simple dipole model[2] for the purposes of simulation. In flight, the satellite body components of this vector can be measured with a magnetometer. It is also possible to use the more accurate IGRF model and magnetometer measurements to help determine the satellite's attitude.[3] To simplify the discussion in the rest of this paper the dipole model will be used:

$$\boldsymbol{B}_0 = \nabla\left[\frac{\boldsymbol{R}^T\boldsymbol{M}_e}{R^3}\right] = [\boldsymbol{I} - 3\boldsymbol{R}\boldsymbol{R}^T]\frac{\boldsymbol{M}_e}{R^3} \tag{2}$$

where

∇ = vector gradient operator
R = radius vector magnitude
$\boldsymbol{R}$ = unit vector along radius
I = Identity matrix
$\boldsymbol{M}_e$ = vector geomagnetic strength of dipole

In the orbital coordinates this model is expressed as

$$\boldsymbol{B}_0 = \begin{bmatrix} B_{X0} \\ B_{Y0} \\ B_{Z0} \end{bmatrix} = \begin{bmatrix} \sin i \cdot \cos\alpha \\ \cos i \\ 2\sin i \cdot \sin\alpha \end{bmatrix}\frac{M_e}{R^3} \tag{3}$$

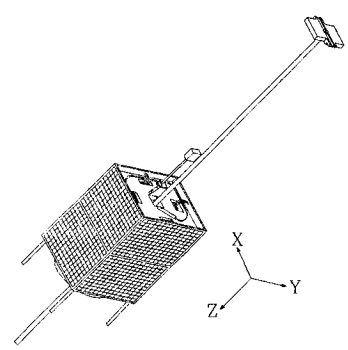

Fig. 1 Typical small satellite.

Received Feb. 14, 1992; revision received Oct. 8, 1993; accepted for publication Oct. 15, 1993.

*Senior Lecturer, Department of Electronic Engineering.

where
i = orbit inclination
α = orbit angle as measured from the ascending node

From this model it can be calculated that a sun-synchronous low Earth orbit (LEO) ($i \approx 99$ deg and altitude ≈ 800 km) presents a small constant B_{Y0} component of 3.3 μT, a maximum B_{X0} component of 21.2 μT over the equator with B_{Z0} zero, and a maximum B_{Z0} component of 42.4 μT over the polar region with B_{X0} zero. The geomagnetic vector therefore rotates inertially twice per polar orbit, almost within the orbital plane. (Note that the $X_0Y_0Z_0$ axes set rotates inertially once per orbit.)

Previous Attempts

The only known (to the author) three-axis stabilization control algorithm for a similar configuration (passive gravity gradient with active magnetorquing) was derived by Martel et al.[3] Their algorithm tends to choose the "most favorable" magnetorquing direction at any control instant by interleaving or simultaneously switching any of the three magnetic coils, relying on the current direction of the local geomagnetic field vector. Their most favorable magnetorquing vector unfortunately does not exclude the generation of unfavorable cross disturbances. This will be explained quickly by means of an example.

First their algorithm. The control error on all three axes is expressed as a Proportional and Derivative (PD) error correction vector $\boldsymbol{e}$:

$$\boldsymbol{e} = \boldsymbol{K}_p\boldsymbol{a} + \boldsymbol{K}_d\boldsymbol{a}' \tag{4}$$

where
K_p = proportional gain matrix
K_d = derivative gain matrix
$\boldsymbol{a}$ and $\boldsymbol{a}'$ = attitude and rate error vectors, respectively
The most favorable magnetorquing vector $\boldsymbol{M}$ is then

$$\boldsymbol{M} = (\boldsymbol{e} \times \boldsymbol{B})/|\boldsymbol{B}| \tag{5}$$

where

$\boldsymbol{B}$ = local body field vector from a magnetometer

The actual torque $\boldsymbol{N}$ then applied to the satellite is obtained from Eq. (1).

For example, if the satellite is three-axis stabilized with zero roll and yaw attitude error but only a pitch error, and assuming that the local geomagnetic field vector contains components in all three body axis, then

$$\boldsymbol{e} = \theta_{err} \cdot \boldsymbol{y} \quad \text{and} \quad \boldsymbol{B} = B_X \cdot \boldsymbol{x} + B_Y \cdot \boldsymbol{y} + B_Z \cdot \boldsymbol{z}$$

Thus,

$$\boldsymbol{M} = (\theta_{err} b_z) \cdot \boldsymbol{x} - (\theta_{err} b_x) \cdot \boldsymbol{z}$$

and

$$\boldsymbol{N} = \theta_{err}[(b_x B_Y) \cdot \boldsymbol{x} - (b_z B_Z + b_x B_X) \cdot \boldsymbol{y} + (b_z B_Y) \cdot \boldsymbol{z}]$$

The second term in the previous equation delivers the desired torque to correct the pitch error, but the first term disturbs the roll and the third term the yaw dynamics directly.

II. Satellite Dynamics

The attitude of the satellite is defined as an ordered series of right-hand positive rotations from the $X_0Y_0Z_0$ orbital axes to the XYZ body axis (see Fig. 2). The first rotation is pitch around the Y_0 axis; this defines a pitch angle θ. After the first rotation, the $X_0Y_0Z_0$ axes form the intermediate LY_0Z' set of axes. The next rotation is roll around the L axis; this defines a roll angle ϕ. After the second rotation, the LMZ axes are formed. The last rotation is yaw around the Z axis; this defines a yaw angle ψ. This set of rotations results in the 2-1-3 Euler transformation to get from orbital to satellite body vector components. After the first two rotations, the LMZ body axes are defined as the nonspinning reference set, used to obtain the angular equations of motion for the roll (L) axis, the near-pitch (M) axis, and the yaw (Z) axis.

Following the derivation of Hodgart[4] and Newton's laws of rotational motion, for a gravity gradient stabilized spacecraft with equal moments of inertia around the X and Y body axis ($I_X = I_Y = I_T$), with a boom and tip mass deployed along the Z axis,

Around the L axis (roll):

$$N_L = \phi'' I_T - (\omega_0 - \theta')C\phi[\omega_z I_Z - (\omega_0 - \theta')S\phi I_T] + 3\omega_0^2 S\phi C\phi C\theta C\theta(I_T - I_Z) \tag{6a}$$

Around the M axis (near pitch):

$$N_M = \theta'' C\phi I_T + \phi'[2(\omega_0 - \theta')S\phi I_T - \omega_z I_Z] + 3\omega_0^2 S\theta C\theta C\phi(I_T - I_Z) \tag{6b}$$

Around the Z axis (yaw):

$$N_Z = \psi'' I_Z - \theta'' S\phi I_Z + \phi'(\omega_0 - \theta')C\phi I_Z \tag{6c}$$

with

$$\omega_z = \psi' + (\omega_0 - \theta')S\phi \tag{6d}$$

where
ω_0 = orbital rate
C = cosine function
S = sine function
N = external torques around LMZ axes
I = moments of inertia around LMZ axes

For small pitch and roll angles (near Earth pointing), when $I_T \gg I_Z$ (boom deployed) and ignoring all of the small coupling terms, these equations can be linearized as follows:

$$\text{Roll: } T_\phi = N_L/I_T = \phi'' + \omega_\phi^2\phi \qquad \{\omega_\phi = 2\omega_0\} \tag{7a}$$

$$\text{Pitch: } T_\Theta = N_M/I_T = \theta'' + \omega_\theta^2\theta \qquad \{\omega_\Theta = \sqrt{3}\omega_0\} \tag{7b}$$

$$\text{Yaw: } T^\psi = N_Z/I_Z = \psi'' \tag{7c}$$

The linearized pitch and roll models, under the influence of gravity gradient, are therefore simple harmonic oscillators at $\sqrt{3}$ and 2 times the orbital rate, respectively; these oscillations

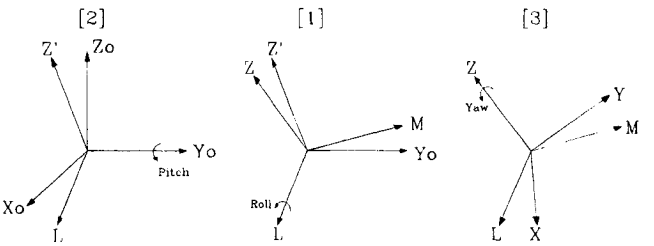

Fig. 2 2-1-3 Euler rotations.

are called libration. The yaw model is a characteristic double integrator inertial system.

When magnetorquing is used as the only active means of controlling the attitude, the control torques in roll, near-pitch, and yaw (*LMZ* axes) can be obtained from Eq. (1) as follows:

$$\text{Roll: } rN_L = M_M \cdot B_Z - M_Z \cdot B_M \tag{8a}$$

$$\text{Pitch: } N_M = M_Z \cdot B_L - M_L \cdot B_Z \tag{8b}$$

$$\text{Yaw: } N_Z = M_X \cdot B_Y - M_Y \cdot B_X \tag{8c}$$

where

$$M_L = M_X \cos \psi - M_Y \sin \psi$$
$$M_M = M_X \sin \psi + M_Y \cos \psi$$

(The variables B_L and B_M are computed similarly from B_X and B_Y.)

The variables B_X, B_Y, and B_Z can be measured by an onboard magnetometer or obtained indirectly from an IGRF model if the satellite's attitude is known.

Control restrictions for a polar LEO

The variables B_X and B_Y (B_L) dominate over the equatorial region due to the strong B_{X0} field component, and the X/Y magnetorquers can be used for yaw control or the Z magnetorquer for pitch control. Over the polar regions B_Z dominates due to the strong B_{Z0} component. Pitch or roll control is therefore possible using M_X/M_Y. The variable B_M will always be small due to a small B_{Y0} component, and a limited use for roll control, when using M_Z over the polar regions, might be possible.

Because of a large I_T/I_Z ratio with a deployed boom (typical 100:1), it is clear from Eqs. (7) that the yaw control loop will be much more sensitive to magnetorquing. When the X/Y magnetorquers are used to control around the pitch and roll axes, extreme care must be taken not to disturb the yaw loop. This can be avoided by using the Z magnetorquer mainly. Pitch error control will be possible, but roll error control will be too heavily restricted. The main objective of any control algorithm will be to make optimal use of M_X, M_Y, and M_Z to effectively damp any pitch and roll libration, while maintaining a yaw angle or rate set point. This has to be done in minimum time with the least amount of control energy, a typical optimal control problem.

III. Fuzzy Controller and Its Analysis

To allow for the choice of the magnetorquer coil that will achieve the best results, given the local geomagnetic field vector and using a well-structured approach, the next algorithm based on fuzzy control rules was designed. Fuzzy logic is defined by Zadeh[5] as follows: "A kind of logic using graded or qualified statements rather than ones that are strictly true or false. The results of fuzzy reasoning are not as definite as those derived by strict logic, but they cover a larger field of discourse."

The intention of this controller design was to define a set of control rules and to implement them in such a way as to make the boundaries between them less strict, resulting in a more flexible system. A variation of the multi-input and single-output (MISO) fuzzy controller of Sugeno and Nishida[6] was implemented. A block diagram of the proposed fuzzy controlled system is shown in Fig. 3. The controller actually consists of three MISO fuzzy control laws, one for each magnetorquer (M_X, M_Y, and M_Z coils). Each control law embodies a fuzzy rule base to decide on the control desirability and output level when using the corresponding torquer. A choice is then made to use the most favorable torquer during the next control interval.

The input variables for the fuzzy controllers are the measured state variables of the satellite and the estimated control torques. This choice of input variables will make it possible to regulate the state variables while considering the control torque constraints (e.g., availability and cross disturbances). The torques can be estimated using Eqs. (8) and the magnetometer readings. A total of six inputs were used:

x_1, x_2 = pitch and roll rate
x_3 = yaw axis control error, see Eqs. (10)
x_4, x_5, x_6 = pitch roll, and yaw torque possible with the specified magnetorquer

These variables are then mapped into fuzzy sets (e.g., P for positive, N for negative, and Z for zero). The fuzzy set values are obtained from membership functions, e.g.,

$$x_1 \rightarrow m_P(x_1) \quad \text{and} \quad x_4 \rightarrow m_N(x_4)$$

The membership functions used for each input variable are shown in Fig. 4. The reasons for choosing the functions in this specific format were multiple, but the most important reason was to limit the number of fuzzy sets but still to obtain a linear mapping in the normal operating region of the system. The amount of overlap between the different fuzzy sets was optimized through simulation and its influence analyzed (see Fig. 5). The saturation point (scaling) of each input variable was done using engineering knowledge of the system and optimized using simulation trials. All inputs are grouped into two fuzzy sets: positive P and negative N. The yaw control torque is supplemented with an extra set: zero Z. This is used in the rules to minimize the disturbance effect to the sensitive yaw control loop.

A fuzzy rule base was constructed from a few simple linguistic rules. Each rule maps to a crisp binary output variable (+1 or −1). The output variable indicates the desired magnetorquer polarity. The M_X and M_Y fuzzy controllers are used for pitch, roll, and yaw control, and they need all six inputs (x_1 to x_6). A set of 12 rules, listed in Table 1, were defined for these controllers. The M_Z controller is used only for pitch and roll control, and only four inputs (x_1, x_2, x_4 and x_5) are used. A set of eight rules are defined as shown in Table 2. As an example, take rule R^2 from Table 1:

R^2: IF x_1 = P AND x_4 = N AND x_6 = Z, THEN u = + 1.

If the pitch rate is positive, if the estimated pitch torque obtainable with X/Y torquer coil (computed as if switched on positively) is negative, and if the estimated yaw torque (disturbance) is close to zero, then the torquer polarity must be positive.

The rule consequent (truth value) is then inferred using correlation-product encoding, the conjunctive (AND) combination of the antecedent fuzzy sets. For rule 2:

$$R^2: \quad \mu^2 = m_P(x_1) \cdot m_N(x_4) \cdot m_Z(x_6).$$

The correlation-product norm is used rather than the more common correlation-minimum norm[7] to enable all rule conditions to contribute to the rule consequent. These truth values are then used to scale the binary output to obtain the rule output:

$$R^2: \quad y^2 = \mu^2 \cdot u.$$

All of the rule outputs is then combined disjunctively (OR) to obtain the crisp rule base output:

$$y = \vee(y^i) = \text{sgn}\left(\sum_{i=1}^{N} y^i\right) \cdot \min\left(1, \left|\sum_{i=1}^{N} y^i\right|\right) \tag{9}$$

The disjunction method of Eq. (9) can be described as a kind of signed Lukasiewicz OR logic. It is chosen to maximally negatively correlate the rule outputs. For example, opposing rule outputs (different in sign) can cancel one another to deliver a small rule base output, thus minimizing the level of cross disturbance.

The fuzzy controller with the largest absolute rule base output is then the preferred one to use in controlling the attitude/rate

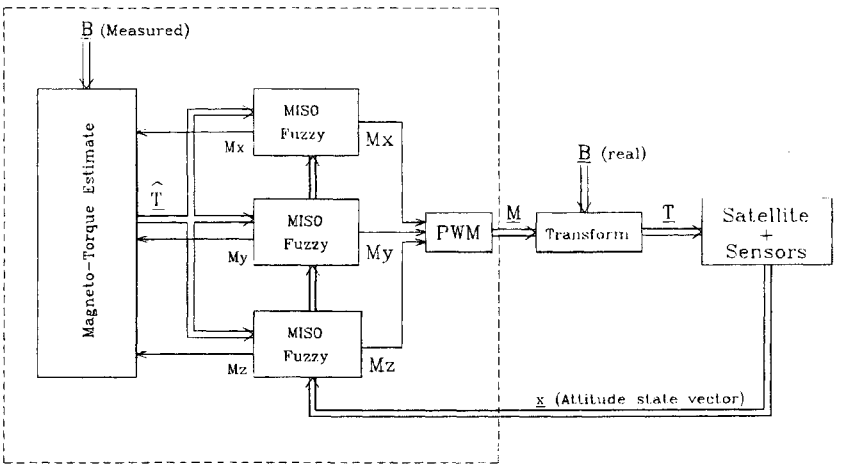

Fig. 3 Block diagram of the fuzzy controller.

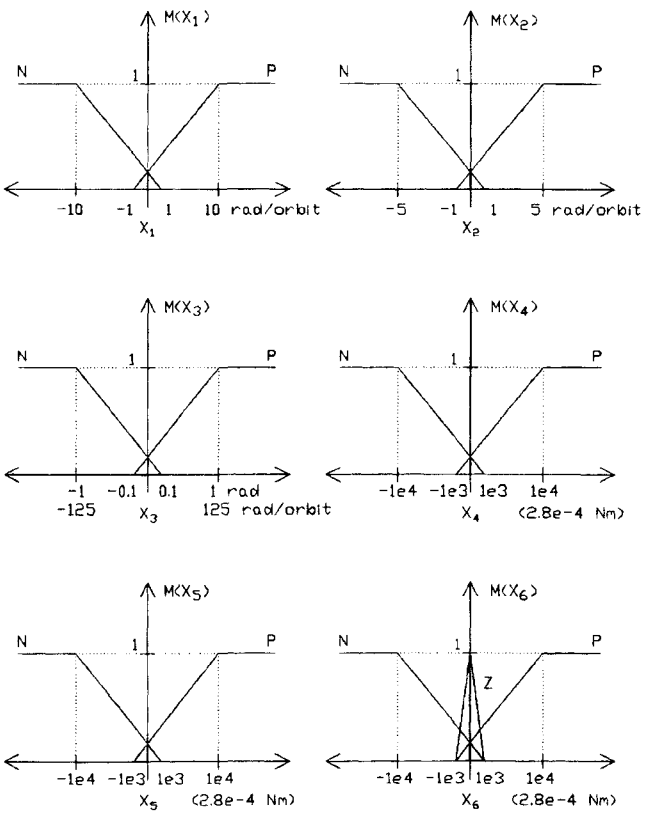

Fig. 4 Fuzzy variable membership functions.

Table 1 M_x and M_y fuzzy variable control rules

Rule	x_1	x_2	x_3	x_4	x_5	x_6	u
R^1	P	—	—	P	—	Z	−1
R^2	P	—	—	N	—	Z	+1
R^3	N	—	—	P	—	Z	+1
R^4	N	—	—	N	—	Z	−1
R^5	—	P	—	—	P	Z	−1
R^6	—	P	—	—	N	Z	+1
R^7	—	N	—	—	P	Z	+1
R^8	—	N	—	—	N	Z	−1
R^9	—	—	P	—	—	P	−1
R^{10}	—	—	P	—	—	N	+1
R^{11}	—	—	N	—	—	P	+1
R^{12}	—	—	N	—	—	N	−1

Table 2 M_z fuzzy variable control rules

Rule	x_1	x_2	x_4	x_5	u
R^1	P	—	P	—	−1
R^2	P	—	N	—	+1
R^3	N	—	P	—	+1
R^4	N	—	N	—	−1
R^5	—	P	—	P	−1
R^6	—	P	—	N	+1
R^7	—	N	—	P	+1
R^8	—	N	—	N	−1

error. Furthermore, the control amplitude (the duration of the magnetorquing pulse, i.e., a pulse width modulation method is used) and sign are also obtainable from the output variable. This variable is directly related to the attitude/rate error and the control torque availability through the choice of the membership functions. The disturbance to the sensitive yaw control dynamics ($I_Z \ll I_T$) is limited by the fuzzy set Z when the pitch and roll rules are evaluated. Further conflicts are implicitly resolved through the summation in Eq. (9).

The optimality and performance (e.g., control response time) of this controller are therefore solely dependent on the choice of the membership functions. Sound engineering judgment and simulation trails were used to achieve these goals. A few examples of these engineering choices follow:

1) A complicating factor was how to insure smaller control pulses for the yaw angle/rate X/Y magnetorquer, while still

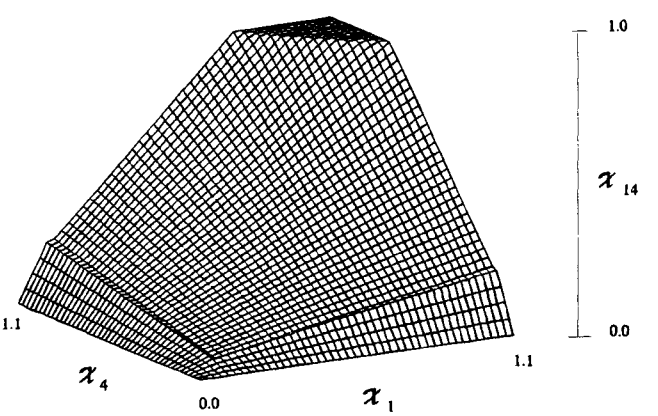

Fig. 5 Positive-positive control surface for the pitch product pair.

weighing the rules equally between pitch, roll, and yaw errors. This was done by a separate summation of rules 1–8 (pitch and roll rules) and rules 9–12 (yaw rules) and then a comparison of the results. If the latter is the greater, the main control effort must preferably be for the yaw loop, and the control effort is scaled down for the more sensitive yaw dynamics.

2) The estimated pitch and roll rate values are used in the fuzzy controllers to implement a rate feedback regulator. The yaw control loop uses, depending on the control function (angular or rate tracking), the following expressions for the yaw control error variable x_3 at sampling instant k:

$$\text{Angle: } x_3(k) = K_{p1}\{[\psi_{\text{ref}}(k) - \psi(k)] - K_d\psi_z(k)\} \tag{10a}$$

$$\text{Rate: } x_3(k) = K_{p2}[\omega_{\text{ref}}(k) - \omega_z(k)] \tag{10b}$$

where

K_{pi} = proportional gains
K_d = derivative gains
ψ_{ref}, ω_{ref} = reference values for yaw angle and yaw rate, respectively
ψ, ω_z = estimator yaw angle and yaw rate values, respectively

The gains K_{pi} and K_d were chosen to satisfy certain transient specifications during the reference commands. Although it may seem strange to implement this linear control method within a nonlinear fuzzy environment, it performed excellently due to the relative small torques needed for yaw maneuvers. The control action after a step change can be completed within a few minutes using the magnetorquers, whereas the magnetic field vector does not change much; its direction will stay favorable during the control effort.

Fuzzy Controller Analysis

The stability and nonlinearity of the fuzzy controller can be analyzed by transforming the linguistic rule base and membership functions to algebraic equations. From Eqs. (7a) and (7b) it follows that the open-loop linearized model for pitch and roll dynamics is oscillatory: pitch and roll librations will be excited due to external disturbance torques. The purpose of a stable control law will be to damp these oscillations using the magnetorquers. If the resulting pitch and roll torques can be proportional, but opposite in sign to the libration rates, the necessary damping will take place. For example, if

$$T_\Theta(t) = -k \cdot \theta' \qquad (k > 0)$$

then, using Eq. (7a),

$$\Theta(s) = \frac{1}{s^2 + ks + \omega_\Theta^2}$$

Depending on the magnitude of k, the closed-loop pitch libration model will have either real or complex, but always stable, left-half s-plane poles. To insure a correct torque sign (opposite to the rate value), the product of a scaled version of the rate and estimated torque around a specific attitude axis can be evaluated. This is done using the membership functions (scaling), the rule base (pairing of rates and torques), and the correlation-product conjunction of the rules. The torques are estimated as if a specific magnetorquer is switched on positively, i.e., the computed evaluation of Eq. (8). If the rate / torque product is positive, the magnetorquer polarity needs to be reversed, or else it was chosen correctly. It can easily be shown that, without any overlap between the P and N fuzzy sets and within the linear mapping range ($x_i \rightarrow m_{\text{P/N}}(X_i) < 1$), the fuzzy controllers simplify to the following algebraic equations:

$$M_{X/Y} = -(\chi_1\chi_4 + \chi_2\chi_5)\xi - \chi_3\chi_6 \tag{11a}$$

$$M_Z = -\chi_1\chi_4 - \chi_2\chi_5$$

where

χ_i = scaled versions of the input variables
$\chi_1\chi_4$, $\chi_2\chi_5$, $\chi_3\chi_6$ = product pairs for pitch, roll, and yaw control
ξ = $1 - 10\,|\chi_6|$ when $|\chi_6| < 0.1$
ξ = 0 when $|\chi_6| > 0.1$
ξ = weighting factor to insure small disturbances around the yaw axis

The dominant product pair (best axis to control) will be the major contributing term in Eqs. (11a) and (11b). It will therefore determine the correct sign and output level for each magnetorquer. Furthermore, the best (highest output level) magnetorquer will be selected from the three possibilities. All of this will insure a dominant stable controlling effort with minimization of the possible cross disturbances.

Libration damping is not needed for the yaw axis but rather a stable feedback control law to regulate either a reference yaw angle or rate. From the choice of x_3 in Eqs. (10a) and (10b) follows a stable control law when the yaw control torque is proportional but opposite in sign to x_3. Using Eq. (7c), a linear continuous model for the yaw control loop will be as follows:

$$\text{Angle: } T_\psi(t) = -k \cdot x_3 = k \cdot K_{p1}[\psi_{\text{ref}}(t) - \psi(t)] - k \cdot K_{p1} \cdot K_d \cdot \omega_z(t) \qquad (k > 0)$$

then

$$\frac{\Psi(s)}{\Psi_{\text{ref}}(s)} = \frac{kK_{p1}}{s^2 + kK_{p1}K_dS + kK_{p1}}$$

and

$$\text{Rate: } T_\psi(t) = -k \cdot x_3 = k \cdot K_{p2}[\omega_{\text{ref}}(t) - \omega_z(t)] \qquad (k > 0)$$

then

$$\frac{\Omega_z(s)}{\Omega_{\text{ref}}(s)} = \frac{kK_{p2}}{s + kK_{p2}}$$

The sign of the yaw product pair will define the magnetorquer polarity in a similar way as in the pitch and roll case. The closed-loop poles of the yaw dynamics will then be stable, and the product level k plus K_{p1}, K_d, and K_{p2} will determine the closed-loop response.

When the P and N fuzzy sets overlap, the scaled versions of the input variables can be rewritten as follows (e.g., for 10% overlap):

$$\text{P: } m_{\text{P}}(\chi_i) = \chi_i + 0.1 \qquad \{-0.1 < \chi_i < 0.9\}$$

$$\text{N: } m_{\text{N}}(\chi_i) = -\chi_i + 0.1 \qquad \{-0.9 < \chi_i > 0.1\}$$

and

$$m_{\text{P/N}}(\chi_i) = 1 \qquad \{|\chi_i| \geq 0.9\}$$

Within the linear mapping range $[m_{P/N}(\chi_i) < 1]$ the fuzzy controllers simplify to similar algebraic equations as in Eqs. (11a) and (11b). However, the product pairs $\chi_1\chi_4$, $\chi_2\chi_5$, and $\chi_3\chi_6$ now become different expressions in the scaled variables, depending on whether the input variables map inside or outside of the overlapping region. The expression to substitute for the pitch product pair is

$$\begin{aligned}
\chi_{14} &= \chi_1\chi_4 + 0.1\,\chi_1 \cdot \mathrm{sgn}(\chi_1) + 0.1\chi_4 \cdot \mathrm{sgn}(\chi_4) - 0.01 && \{|\chi_1| \geq 0.1,\ |\chi_4| \geq 0.1\}\\
&= 2\chi_1\chi_4 + 0.2\chi_4 \cdot \mathrm{sgn}(\chi_1) && \{|\chi_1| \geq 0.1,\ |\chi_4| < 0.1\}\\
&= 2\chi_1\chi_4 + 0.2\chi_1 \cdot \mathrm{sgn}(\chi_4) && \{|\chi_1| < 0.1,\ |\chi_4| \geq 0.1\}\\
&= 4\chi_1\chi_4 && \{|\chi_1| < 0.1,\ |\chi_4| < 0.1\}
\end{aligned}$$

The previous expression can easily be derived from the four rules in each rule base pertaining to the pitch-based input variables (x_1 and x_4), e.g., rules 1–4 in Table 2. The control surface of the pitch product pair in the positive-positive quadrant (both input variables are positive) is shown in Fig. 5. The negative-negative quadrant control surface looks similarly, whereas the positive-negative and negative-positive control surfaces have a negative output result. It is important to notice that the overlapping of the membership functions not only preserves the correct product pair sign (important for stability) but also increases the output (magnetorquer level) for small input values. This tends to improve the sensitivity and response of the control system to small error signals without unduly complicating the controller implementation.

IV. Multiinput Multiouput Linear Quadratic Regulator

The linearized, uncoupled equations of Eqs. (7) were converted to discrete state-space form to obtain a satellite model for the attitude controller:

$$\begin{aligned}
\boldsymbol{x}(k+1) &= \boldsymbol{\Phi x}(k) + \boldsymbol{\Gamma}_1\boldsymbol{T}(k)\\
\boldsymbol{y}(k+1) &= \boldsymbol{H x}(k+1)
\end{aligned} \tag{12}$$

where

$$\boldsymbol{y}(k) = [\theta(k),\ \theta'(k),\ \phi(k),\ \phi'(k),\ \psi(k),\ \psi'(k)]^T$$

The torque vector $\boldsymbol{T}(k)$ is related to the magnetic dipole vector $\boldsymbol{M}(k)$ through a nonlinear, time-varying relationship depending on the geomagnetic field vector $\boldsymbol{B}_0$ and the satellite's attitude. Equations (8) and a 2-1-3 Euler transformation to obtain the body geomagnetic vector $\boldsymbol{B}$ can be used to compute the time-varying matrix $\boldsymbol{\Gamma}_2(k)$ at every sampling instant k.

Then

$$\boldsymbol{T}(k) = \boldsymbol{\Gamma}_2(k)\boldsymbol{M}(k) \tag{13}$$

where

$$\boldsymbol{\Gamma}_2(k) = \text{matrix function } [\boldsymbol{B}_0(k),\ \theta(k),\ \phi(k),\ \psi(k)]$$

If the control input to the model is then taken as $\boldsymbol{M}(k)$, the input matrix becomes

$$\boldsymbol{\Gamma}(k) = \boldsymbol{\Gamma}_1\boldsymbol{\Gamma}_2(k) \tag{14}$$

This results in a time-varying multiinput multioutput (MIMO) state-space model with three inputs (M_X, M_Y, and M_Z) and six state variables. The attitude controller was implemented as a state-space feedback regulator. Linear quadratic regulator theory (LQR) was then used to compute the feedback gain matrix K to minimize the cost functional:

$$J = \frac{1}{2}\sum_{k=0}^{\infty}[\boldsymbol{x}_e^T(k)\boldsymbol{Q}_1\boldsymbol{x}_e(k) + \boldsymbol{M}^T(k)\boldsymbol{Q}_2\boldsymbol{M}(k)] \tag{15}$$

with control law

$$\boldsymbol{M}(k) = -\boldsymbol{K}\boldsymbol{x}_e(k) \tag{16}$$

where

$$\boldsymbol{x}_e(k) = \boldsymbol{x}(k) - \boldsymbol{r}(k)$$

The reference input vector $\boldsymbol{r}(k)$ is assumed to be constant or slowly time varying and is included in the regulator loop as indicated in Fig. 6. The only reference signal actually needed for an Earth-pointing satellite is either a reference yaw angle (zero pitch and roll) when three-axis stabilization is done or a reference yaw rate (with a known roll offset angle due to a gyroscopic torque opposing the gravity gradient torque) when a z spin is needed.

For this infinite time optimization problem, the cost function Eq. (15) can be minimized by solving an algebraic Riccatti equation:

$$\boldsymbol{S}_\infty = \boldsymbol{\Phi}^T[\boldsymbol{S}_\infty - \boldsymbol{S}_\infty\boldsymbol{\Gamma}\boldsymbol{R}^{-1}\boldsymbol{\Gamma}^T\boldsymbol{S}_\infty]\boldsymbol{\Phi} + \boldsymbol{Q}_1 \tag{17}$$

This will give an optimum steady-state feedback gain matrix K:

$$\boldsymbol{K}_\infty = [\boldsymbol{Q}_2 + \boldsymbol{\Gamma}^T\boldsymbol{S}_\infty\boldsymbol{\Gamma}]^{-1}\boldsymbol{\Gamma}^T\boldsymbol{S}_\infty\boldsymbol{\Phi} \tag{18}$$

To solve the Riccatti equation the method of eigenvector decomposition can be used.[8] This entails finding the eigenstructure of the control Hamiltonian matrix:

$$\boldsymbol{H}_c = \begin{bmatrix} \boldsymbol{\Phi} + \boldsymbol{\Gamma}\boldsymbol{Q}_2^{-1}\boldsymbol{\Gamma}^T\boldsymbol{\Phi}^{-T}\boldsymbol{Q}_1 & -\boldsymbol{\Gamma}\boldsymbol{Q}_2^{-1}\boldsymbol{\Gamma}^T\boldsymbol{\Phi}^{-T} \\ -\boldsymbol{\Phi}^{-T}\boldsymbol{Q}_1 & \boldsymbol{\Phi}^{-T} \end{bmatrix} \tag{19}$$

In this application, however, the input matrix $\boldsymbol{\Gamma}(k)$ is time varying, and the steady-state feedback matrix $\boldsymbol{K}_\infty$ only applies to a linear time-invariant plant. To apply LQR theory to a time-varying plant one has to solve backwards in time a dynamic Riccati equation to obtain the time-varying feedback matrix $\boldsymbol{K}(k)$. However, this will only apply to plants where the future plant variations are perfectly known a priori. Unfortunately, future $\boldsymbol{\Gamma}(k)$ matrices are unknown without knowledge of $\boldsymbol{K}(k)$, the reason being that $\boldsymbol{\Gamma}(k)$ is also a function of the attitude and therefore affected by the control law itself [dependent on previous $\boldsymbol{K}(k)$ values].

It was decided to implement a steady-state LQR design every sampling period. This is a well-known practice in the adaptive control field[9] whenever the plant is very slowly time varying.

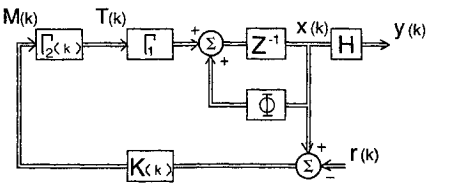

Fig. 6 MIMO regulator loop.

The open-loop dynamics (eigenvalues) in this application are time invariant, and only the control input matrix will affect the plant's controllability with time. Figure 7 indicates how the controllability is affected with time during a typical simulation. The minimum singular value of the controllability matrix is shown; whenever this value becomes zero, one of the open-loop modes becomes uncontrollable. It is further obvious that a dominant cyclic change in controllability occurs twice per orbit due to the geomagnetic field vector direction. The lowest values are over the equatorial region when the roll dynamics become weakly controllable due to the small B_{Y0} component. Although the field direction changes at about the same rate as the satellite's libration dynamics (ω_θ and $\omega_\phi \approx 2\omega_0$), a gain scheduled LQR system is found to perform quite well, although it is no longer truly optimal.

It is computationally very demanding to compute $\Gamma(k)$ every sampling period, since the Hamiltonian matrix is of twice the state-space model order; e.g., 12 eigenvalues have to be found and the corresponding 6 eigenvectors of the stable eigenvalues of matrix H_c. The solution of the Riccatti equation S_∞ can then be computed and the gain matrix K_∞ obtained from Eq. (18). If the matrix of eigenvectors V_I associated with the stable eigenvectors (inside the unit circle) is written in block form as

$$V = \begin{bmatrix} X_I \\ \Lambda_I \end{bmatrix} \tag{20}$$

the solution for the Riccati equation is

$$S_\infty = \Lambda_I X_I^{-1} \tag{21}$$

The practical computing steps that have to be performed every sampling period are as follows:

1. Compute the eigenvalues of H_c from Eq. (19) with $\Gamma = \Gamma(k)$.
2. Compute the eigenvectors from the stable eigenvalues and block them as in Eq. (20).
3. Compute S_∞ from Eq. (21) and then K_∞ from Eq. (18).
4. Use $K(k) = K_\infty$ for feedback regulation.

This method insures stable closed-loop eigenvalues (Fig. 8) and minimization of the cost functional J in Eq. (15) every sampling instant to reduce any undesired disturbances and to make "optimal" use of the available magnetorquing energy. The weighing matrix Q_1 is chosen to reflect the relative control accuracy needed for the various state variables. In this application it was chosen as a diagonal matrix with the smallest elements weighing the yaw state variables, due to the less strict accuracy needed for the sensitive yaw loop. Diagonal weighting matrix Q_2 is chosen to reflect the relative importance of the three magnetorquing coils and to determine the controller bandwidth. The Z magnetorquer weight was chosen the smallest to insure it was favored for pitch and roll libration damping, due to a lack of any disturbances in the yaw control loop (around the Z axis).

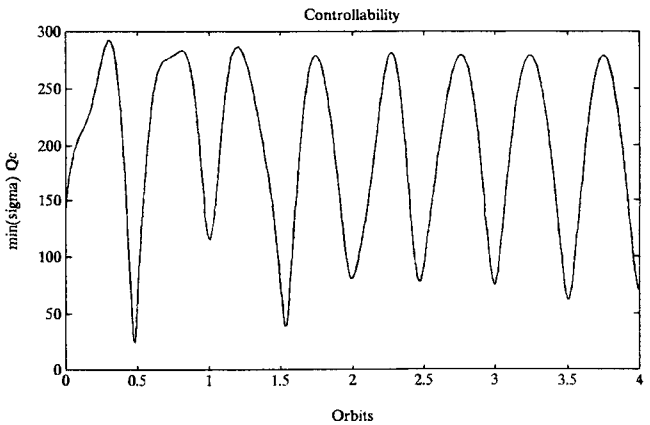

Fig. 7 Controllability variation with time.

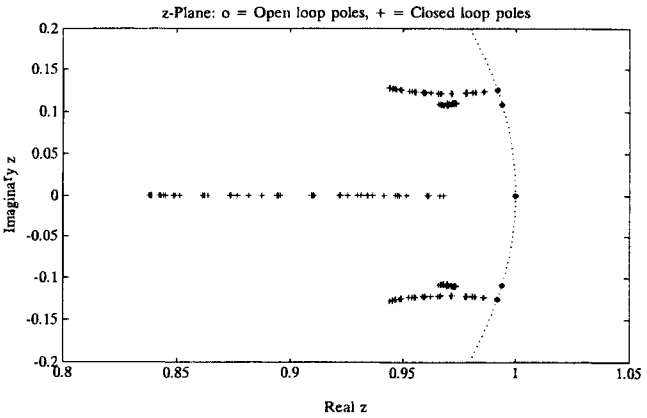

Fig. 8 LQR closed-loop eigenvalue (pole) shift.

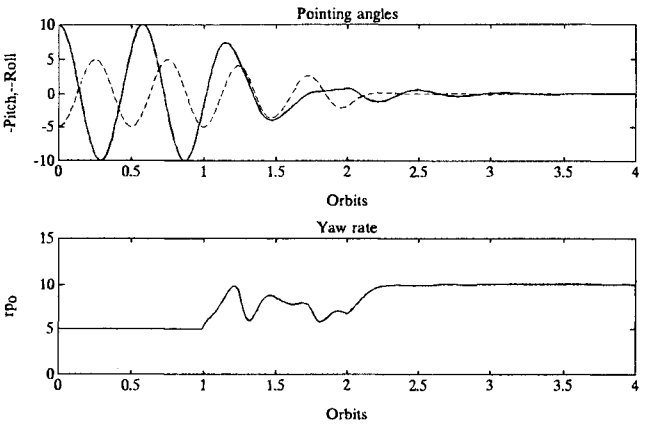

Fig. 9 Ideal MIMO LQR with slack yaw rate control.

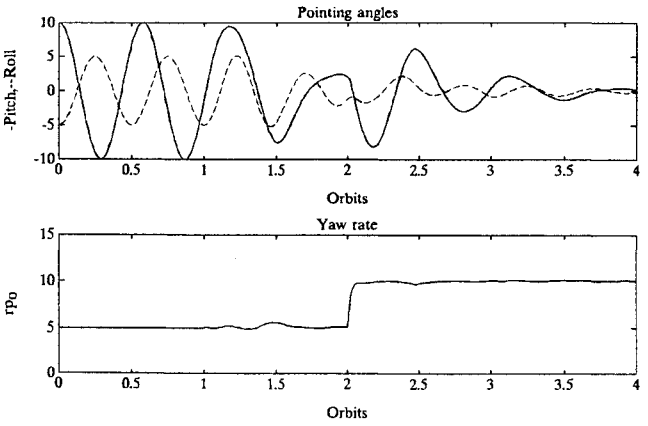

Fig. 10 Ideal MIMO LQR with tight yaw rate control.

V. Simulation Results

To compare the two controller types proposed, the following conditions were adhered to throughout the various simulation trials. The librations were damped from an initial pitch angle of 10 deg and roll angle of −5 deg with zero initial pitch and roll rates. A spinning satellite was assumed at an initial yaw rate of five revolutions per orbit (rpo). During the first orbit no control was done to enable initial estimator attitude tracking. At the start of the second orbit the attitude controller was activated to damp the pitch and roll librations and to maintain the reference yaw rate at 5 rpo. At the start of the third orbit the yaw rate set point was changed to 10 rpo. The simulation

Table 3 Controller on-time comparison

Control law	M_X, min	M_Y, min	M_Z, min	Total, min
Idealized LQR (slack yaw)	1.27	1.39	2.66	5.32
Idealized LQR (tight yaw)	2.08	2.35	6.11	10.54
Realistic LQR (slack yaw)	1.95	1.96	2.82	6.73
Realistic LQR (tight yaw)	1.81	1.78	5.41	9.00
Realistic fuzzy controller	1.02	0.79	6.24	8.05
Realistic Martel et al. controller	2.57	2.63	2.27	7.47

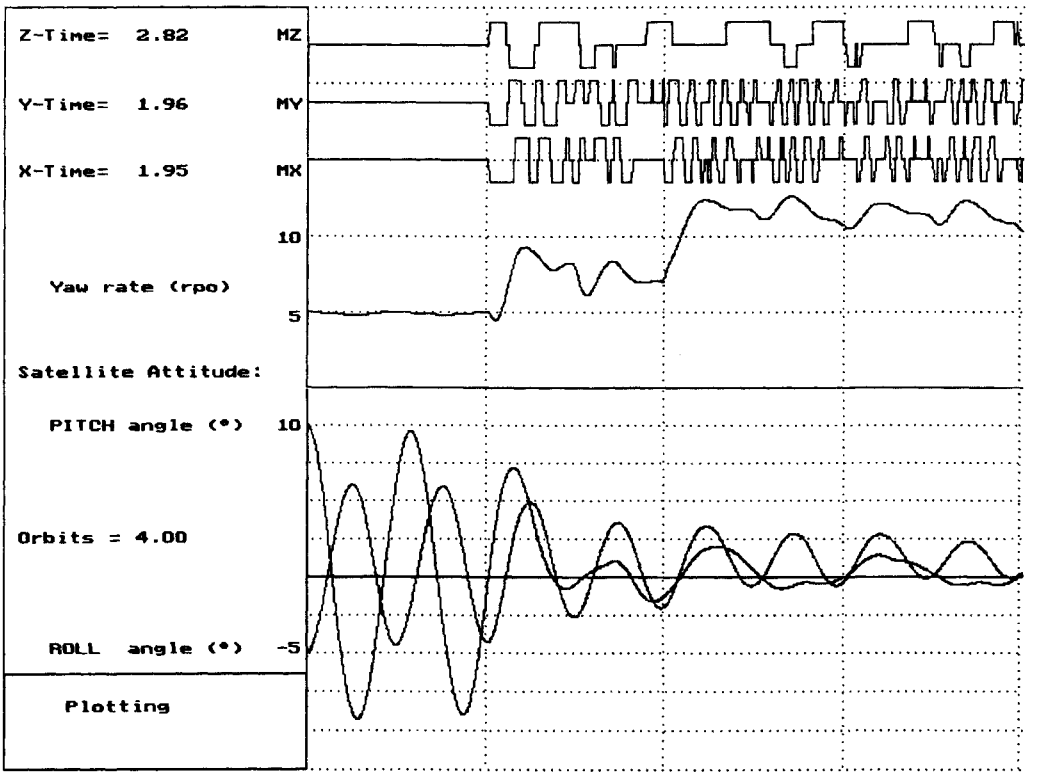

Fig. 11 Realistic MIMO LQR with slack yaw rate control.

runs were terminated at the end of the fourth orbit to compare the libration damping and rate tracking performance and to display the accumulated on-time of the X, Y, and Z magnetorquers. The latter is an indication of the control energy used. The magnetic field dipole model of Eq. (3) was used in all of the simulations to insure similar controllability conditions (torque availability) in all cases.

Figure 9 shows the simulation result obtained under ideal conditions for the adaptive MIMO LQR controller. A linear uncoupled model was used for the satellite dynamics, and exact measurement of the state variables was assumed; no estimators were used or sensor and system noise added. The initial pitch and roll librations were damped almost completely within two orbits. The yaw rate was, however, disturbed during the main libration damping effort in the second orbital period. The yaw rate eventually increased to the new reference setpoint of 10 rpo as expected.

Figure 10 was obtained under similar conditions as the previous result, but the relevant weighting factor in Q_1 increased for tighter yaw rate control. The disturbance caused by libration damping is less apparent on the yaw rate, but the opposite effect of disturbances on the pitch and roll control loops during a yaw rate set point change is more prominent. The amount of control energy used has approximately doubled (see Table 3), and the libration damping efficiency has reduced.

Figures 11 and 12 show the simulation results obtained under more realistic conditions for the adaptive MIMO LQR controller. The full nonlinear satellite dynamic model with cross-coupling terms [Eqs. (6a–6d)] were implemented. An aerodynamic disturbance torque that varies between a maximum and minimum value per orbit was added to the model. Linear state estimators were used to extract the attitude information from noisy sensor measurements (noise variation of ± 1 deg maximum). The estimated state variables were then used for LQR feedback. The Q_1 and Q_2 weighting matrices of Figs. 11 and 12 correspond to those used in Figs. 9 and 10, respectively. It is clear that the libration damping was done less effectively than in the previous ideal case. The control energy consumed did, however, stay comparable, as Table 3 indicates.

Figure 13 presents the result when utilizing the fuzzy controller under realistic simulation conditions. The libration damping and yaw rate setpoint tracking outperformed the adaptive MIMO LQR controller. The energy effectiveness of this controller was also marginally better than the LQR implementation. Figure 14 shows the performance of the control algorithm of Martel et al.[3] when subjected to the same conditions as the newly proposed controllers. The unfavorable disturbance to the yaw rate is evident, and the initial libration damping is also less effective compared with the fuzzy controller.

VI. Conclusions

Two new controllers were presented for an attitude control problem where the use of magnetorquing imposes some control constraints: 1) control torque unavailability during certain

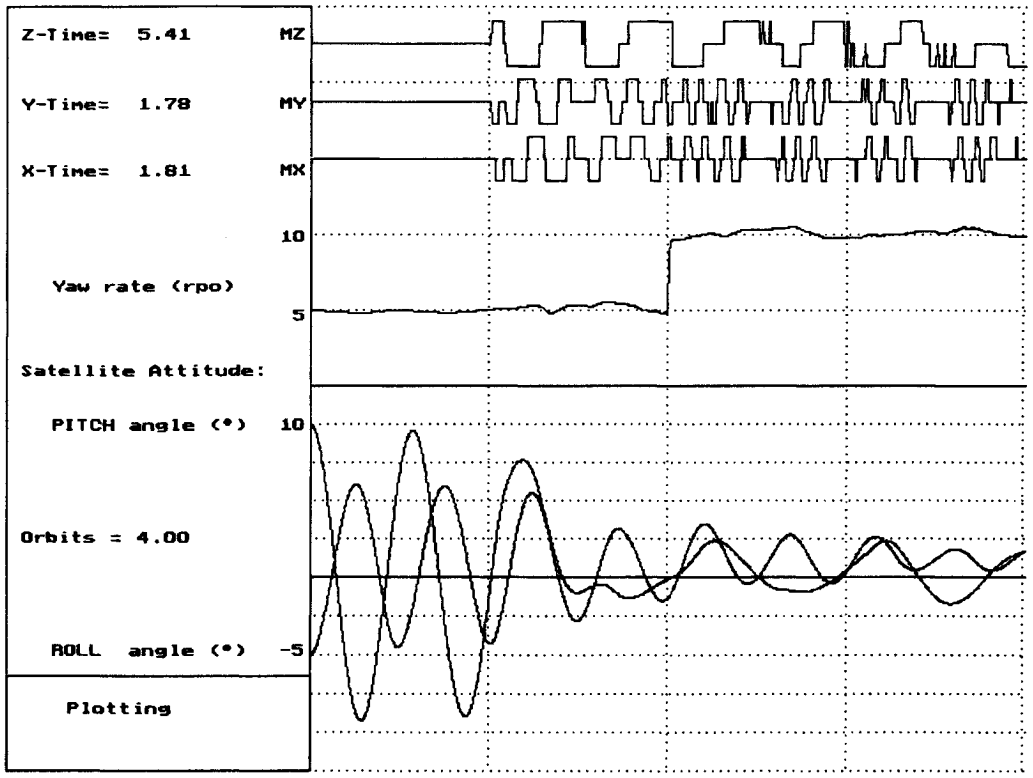

Fig. 12 Realistic MIMO LQR with tight yaw rate control.

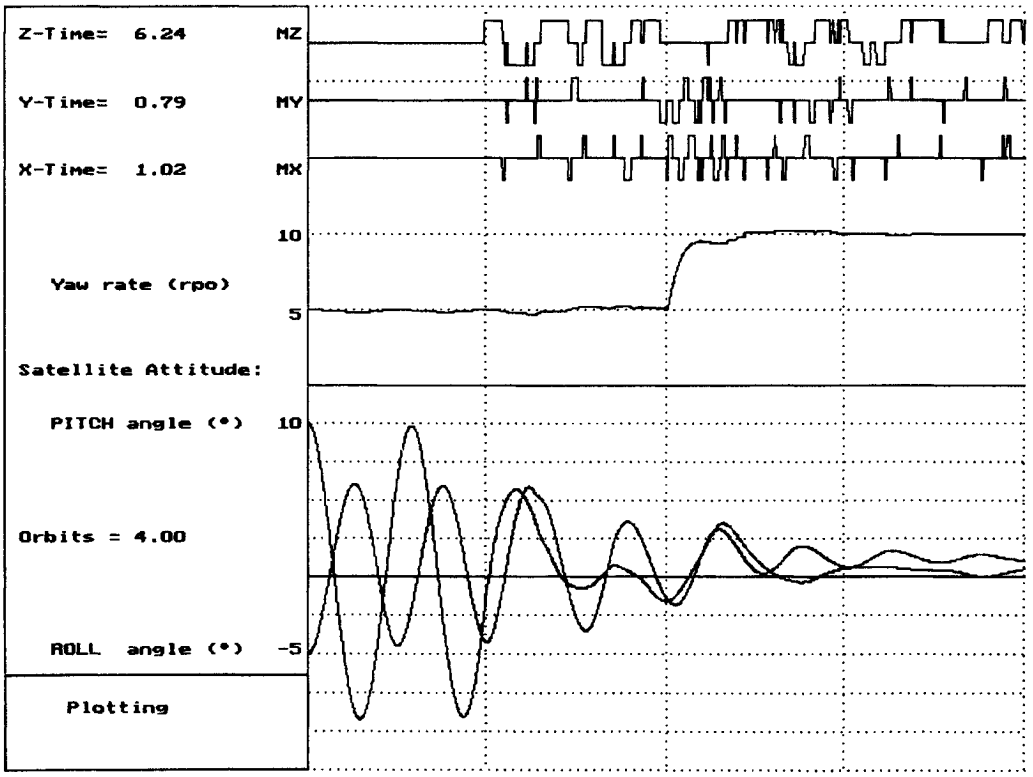

Fig. 13 Fuzzy controller in a realistic environment.

orbital regions and 2) cross-disturbance torques between attitude axes.

The fuzzy controller achieved the best overall libration damping and setpoint tracking with comparable control energy results when tested under various different conditions. This controller is computationally less demanding than the adaptive MIMO LQR controller. The logical and structured manner in which the fuzzy rules and membership functions are chosen and implemented can only lead to an improved understanding of the control problem to be solved. Overlapping of the fuzzy sets helps to shape the control surface of the controller output, in this case to increase the controller sensitivity to small inputs. Proving the stability of some fuzzy controllers can sometimes be difficult if not impossible. However, for this relatively simple

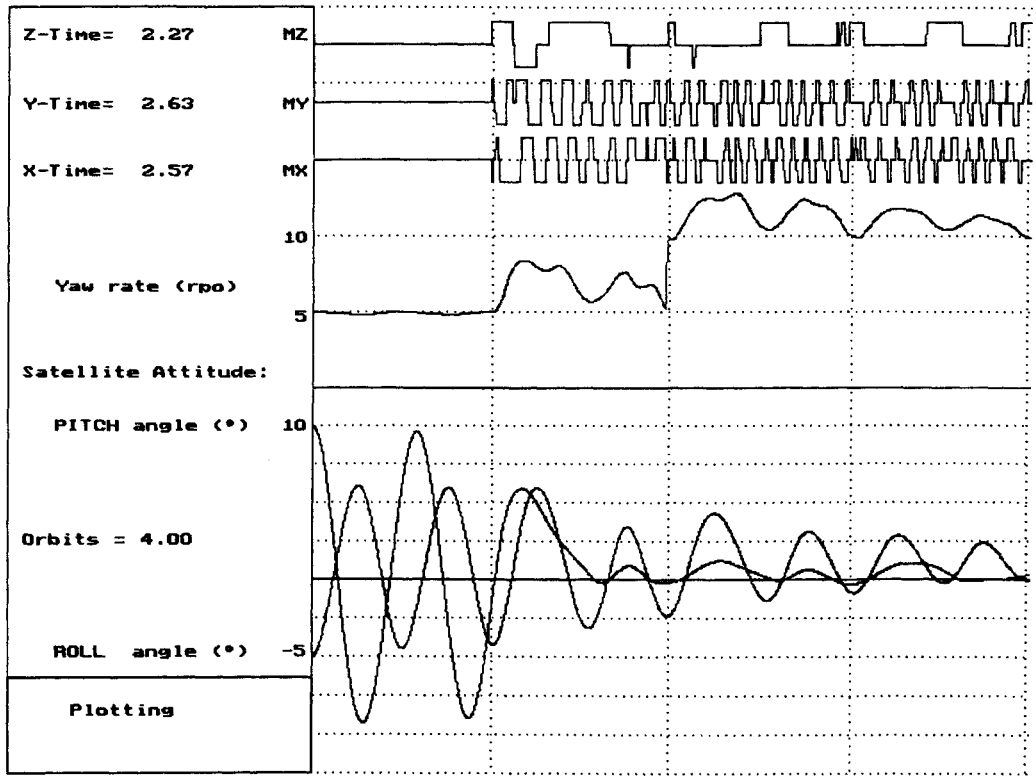

Fig. 14 Martel et al. controller in a realistic environment.

implementation it was possible to reduce the fuzzy controller to a few algebraic equations and to prove the stability through inspection of the damping term. The only possible drawback when designing the fuzzy controller is that, to optimize a specific set of rules and membership functions, no analytical methods are available at present. Sound engineering judgment and various simulation trials are needed.

The MIMO LQR controller is, however, also subject to a certain degree of heuristics when choosing the two weighting matrices Q_1 and Q_2. Especially in this application, various simulation trials were needed to find the "best" weighting factors. This was done not to improve the stability of the system but only to obtain the correct share of control energy to the roll and pitch libration damping loops. Another reason was to reduce the disturbances due to magnetorquing to the sensitive yaw rate loop.

The Martel et al. controller (MPP) offered no adjustment mechanisms to limit the amount of disturbances between the control axis. Its performance over the first three controlled orbits was similar to the MIMO LQR with slack yaw rate control.

An implementation difference between the fuzzy controller and the others worth pointing out is that the fuzzy controller only selects one magnetorquer to be pulsed during each sampling interval; the LQR and MPP controllers normally use all three magnetorquers, and the pulses have to be interleaved if it is impossible to be simultaneously applied.

All of the controllers were able to keep the pointing accuracy of the satellite to within 1 deg once the initial libration energy was removed, although the best final accuracy was achieved with the fuzzy and MPP controllers. The simulations were done over several orbits using attitude sensor noise and a cyclic aerodynamic disturbance torque that will result in a pitch libration amplitude of approximately 1 deg when left uncontrolled. Because of the limitation of pitch control to only certain regions of an orbit, it will not be possible to oppose any disturbance torque continuously. The control actions must, however, attempt not to worsen the disturbance influence. This was successfully achieved with all of the controllers.

References

[1] Wertz, J. R., *Spacecraft Attitude Determination and Control, Astrophysics and Space Science Library,* Vol. 73, D. Reidel Publishing Co., Boston, 1978 (reprinted 1986).

[2] Rodden, J. J., "Closed-Loop Magnetic Control of a Spin-Stabilized Satellite," *Automatica,* Vol. 20, No. 6, 1984, pp. 729–735.

[3] Martel, F., Pal, P. K., and Psiaki, M., "Active Magnetic Control System for Gravity Gradient Stabilized Spacecraft," *Proceedings of 2nd Annual AIAA/USU Conference on Small Satellites,* Utah State Univ., Sept. 1988.

[4] Hodgart, M. S., "Gravity Gradient and Magnetorquing Attitude Control for Low-Cost Low Earth Orbit Satellites—The UoSAT Experience," Ph.D. Dissertation, Univ. of Surrey, Surrey, England, UK, June 1989.

[5] Zadeh, L. A., "Making Computers Think Like People," *IEEE Spectrum,* Aug. 1984, pp. 26–32.

[6] Sugeno, M., and Nishida, M., "Fuzzy Control of a Model Car," *Fuzzy Sets and Systems,* Vol. 16, North-Holland, Amsterdam, The Netherlands, 1985, pp. 103–113.

[7] Kosko, B., *Neural Networks and Fuzzy Systems,* Prentice-Hall, Englewood Cliffs, NJ, 1992, pp. 299–337.

[8] Franklin, G. F., Powell, J. D., and Workman, M. L., *Digital Control of Dynamic Systems,* Addison-Wesley, Reading, MA, 1990, pp. 422–439.

[9] Åström, K. J., and Wittenmark, B., *Adaptive Control,* Addison-Wesley, Reading, MA, 1989, pp. 194–198.